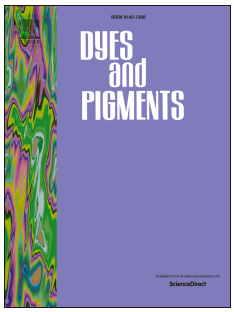

Development of a fluorescent chemosensor for chloride ion detection in sweat using Ag^+-benzimidazole complexes

Jaewon Kim, Suji Lee, Sudeok Kim, Minhyuk Jung, Hohjai Lee, Min Su Han

PII: S0143-7208(19)32715-9

DOI: https://doi.org/10.1016/j.dyepig.2020.108291

Reference: DYPI 108291

To appear in: *Dyes and Pigments*

Received Date: 25 November 2019

Revised Date: 18 February 2020

Accepted Date: 18 February 2020

Please cite this article as: Kim J, Lee S, Kim S, Jung M, Lee H, Han MS, Development of a fluorescent chemosensor for chloride ion detection in sweat using Ag^+-benzimidazole complexes, *Dyes and Pigments* (2020), doi: https://doi.org/10.1016/j.dyepig.2020.108291.

CRediT author statement

Title: Development of a fluorescent chemosensor for chloride ion detection in sweat using Ag^{+}-benzimidazole complexes

- **Jaewon Kim:** Methodology, Investigation, Visualization, Writing – Original Draft
- **Suji Lee:** Methodology, Visualization, Writing – Original Draft
- **Sudeok Kim:** Methodology
- **Minhyuk Jung:** Investigation
- **Hohjai Lee:** Project administration
- **Min Su Han:** Conceptualization, Writing – Review & Editing, Project administration

Graphical Abstract

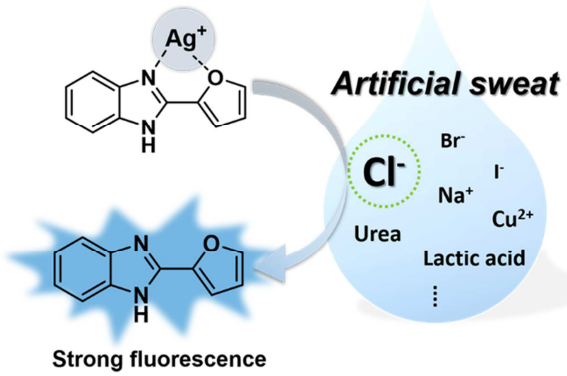

Development of a fluorescent chemosensor for chloride ion detection in sweat using Ag^+-benzimidazole complexes

Jaewon Kim‡, Suji Lee‡, Sudeok Kim, Minhyuk Jung, Hohjai Lee* and Min Su Han*

Department of Chemistry, Gwangju Institute of Science and Technology, 123 Cheomdangwagi-ro, Buk-gu, Gwangju 61005, Republic of Korea

*Corresponding authors. hohjai@gist.ac.kr (H. Lee), happyhan@gist.ac.kr (M. S. Han)

‡ J. K. and S. L. contributed equally to this work.

Abstract

The level of chloride ions (Cl^-) in sweat is a recognized biomarker for the genetic disorder cystic fibrosis (CF). The accurate quantitation of chloride ions in sweat is therefore a vital diagnostic tool for this life-threatening disease. In this work, a fluorescent, chloride ion chemosensor was developed by exploiting the strong interaction between silver (Ag^+) and chloride ions. Using the concept of ligand displacement, six Ag^+-benzimidazole complexes were prepared as candidate chloride ion chemosensors. The Ag^+-2-(Furan-2-yl)-1*H*-benzo[*d*]imidazole (Ag^+-**FBI**) complex was identified as the optimal sensor owing to its Ag^+-**FBI** high sensitivity (limit of detection = 19 μM), short response time (< 3 min), and remarkable fluorescence turn-on response across a broad pH range (pH 6-9). The Ag^+-**FBI** complex exhibited high selectivity for Cl^- ions and was successfully used to quantify chloride ions in artificial sweat samples containing multiple ions and other biological constituents. This unique, simple, and effective probe thus shows great potential for clinical diagnostic applications.

Keywords: *Metal-ligand exchange; Ligand displacement; Chloride ion; Fluorescent chemosensor; Cystic fibrosis; Sweat test*

1. Introduction

Chloride ions (Cl^-) are the most abundant ions in biosystems [1]. They are ubiquitous in agricultural, environmental, industrial, and physiological systems and are extensively used in organic chemicals, agricultural fertilizers, and even as food additives [2-4]. In clinical settings, chloride ions in sweat are used as a biomarker for the genetic disorder cystic fibrosis (CF), which is caused by mutations in the cystic fibrosis transmembrane conductance regulator (*CFTR*) gene [5-9]. The CFTR protein functions as a chloride ion channel and abnormal proteins result in increased levels of chloride ions being present in sweat, making the detection and quantification of sweat chloride an invaluable tool for diagnosing CF [10]. Although several analytical techniques exist for detecting and quantifying chloride ions, including ion chromatography and electroanalytical chemistry methods involving potentiometry and coulometry, they are limited by the accessibility and complexity of the instrumentation [11-16]. A potential alternative to these systems is chemosensors, which benefit from both ease of use and faster detection. Unfortunately, despite the development of multiple chloride ion chemosensors over the past two decades, few have been applicable for the analysis of biological samples owing to the lack of a specific recognition unit for the chloride ion [17-30].

Silver ions (Ag^+) strongly bind to chloride ions ($K_{sp}(AgCl) = 1.77 \times 10^{-10}$), making them a valuable reagent for the specific recognition of chloride ions [31]. The strong interaction between silver and chloride ions was exploited for the development of the established Mohr method for chloride ion detection. This technique is based on precipitation titration of AgCl using silver nitrate ($AgNO_3$) as the titrant and potassium chromate (K_2CrO_4) as the indicator [32,33]. While this method is still widely used to analyze halide ions, it suffers from requirements of large reagent volumes and alkaline working conditions. Despite the limitations of the Mohr method, the strong interaction between silver and chloride ions presents a clear opportunity for the development of a sensitive and selective chemosensor for chloride ion detection.

A great number of chemosensors have been developed using the concept of ligand displacement [34-41]. This design relies on the change in the optical properties of a free and metal-complexed fluorescent or chromogenic dye. Analyte detection is based on the ligand exchange reaction between the metal-dye complex and an analyte with a strong binding affinity for the complexed metal ion. Herein, we developed a selective, fluorescent chemosensor for chloride ions based on ligand displacement from Ag^+-benzimidazole complexes. Six benzimidazole derivatives (**1a**-**1c**, **2a**-**2c**) were synthesized as fluorescent ligands based on previous reports

describing N-heterocycles, and particularly benzimidazoles, as good ligands for silver ions [42-46]. Fluorescence-quenched Ag^+-benzimidazole complexes (Ag^+-**1a**-**1c**, **2a**-**2c**) were prepared and investigated to determine their ability to detect chloride ions via ligand exchange-induced fluorescence recovery (Scheme 1).

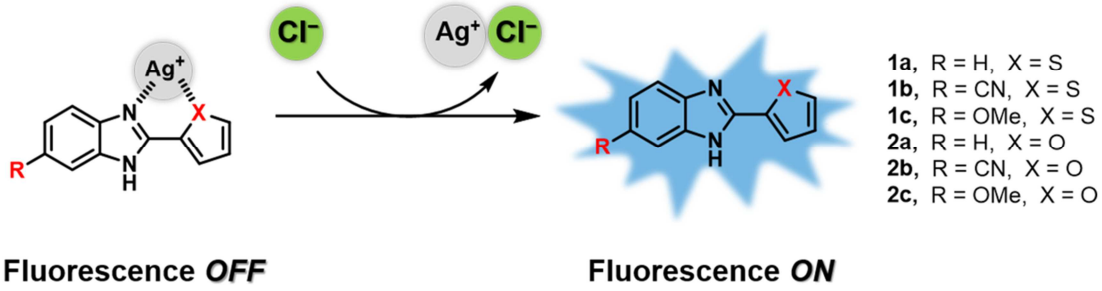

Scheme 1. Chloride ion chemosensor based on ligand displacement from Ag^+-benzimidazole complexes.

2. Experimental

2.1. Materials and instrumentation

Chemical reagents were purchased from commercial sources (Sigma-Aldrich, Alfa Aesar, Duksan, Daejung, and Tokyo Chemical Industry) and, unless otherwise stated, were used without further purification. ^{1}H- and ^{13}C-NMR spectra were recorded on a JEOL 400 MHz NMR spectrometer. Mass spectra were obtained using an Agilent ESI-Q/TOF (quadrupole/time-of-flight) mass spectrometer. Melting points were measured using a BUCHI Melting Point M-565. FT-IR spectra were obtained using a Thermo Scientific Nicolet iS10 FT-IR spectrometer. UV-Vis and preliminary fluorescence spectra were recorded on a BioTek Cytation™ 3 Cell Imaging Multi-Mode Reader. Fluorescence spectra were obtained using an Agilent Cary Eclipse fluorescence spectrophotometer.

2.2. General synthesis and characterization

2.2.1. General procedure for the synthesis of 2-substituted benzimidazoles [47]

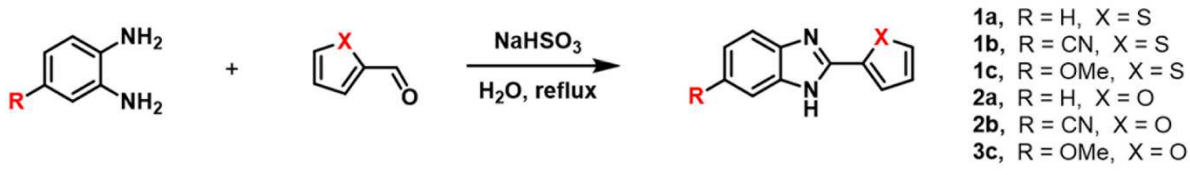

Scheme 2. General synthesis of benzimidazole derivatives (**1a**-**1c**, **2a**-**2c**).

A mixture of aldehyde (10.00 mmol) and $NaHSO_3$ (11.0 equiv., 11.45 g) in H_2O (30 mL) was heated to reflux. A solution of an *o*-phenylenediamine derivative (10.00 mmol) in H_2O (10 mL) was added dropwise to the solution and the reaction was further refluxed. Upon completion, the reaction mixture was cooled to room temperature and the precipitate was collected by vacuum filtration. The residue was washed with H_2O and dried under vacuum.

2.2.2. Characterization of 2-substituted benzimidazoles

*2-(Thiophen-2-yl)-1H-benzo[d]imidazole (**1a**)* [47,48] (1.67 g, 84%) pale yellow solid. mp 327-332 □; ^{1}H-NMR (400 MHz, DMSO-d_6) δ 12.95 (s, 1H), 7.84 (dd, *J* = 3.7, 1.2 Hz, 1H), 7.72 (dd, *J* = 5.2, 1.1 Hz, 1H), 7.56 (q, *J* = 3.0 Hz, 2H), 7.24-7.17 (m, 3H); ^{13}C-NMR (100 MHz, DMSO-d_6) δ 147.6, 139.7, 134.2, 129.3, 128.8, 127.3, 122.7, 115.4.

*2-(Thiophen-2-yl)-1H-benzo[d]imidazole-6-carbonitrile (**1b**)* (0.35 g, 42%) pale yellow solid. mp 245-248 □; ^{1}H-NMR (400 MHz, DMSO-d_6) δ 13.47 (s, 1H), 8.08 (s, 1H), 7.92 (d, *J* = 4.5 Hz, 1H), 7.79 (dd, *J* = 5.0, 1.0 Hz, 1H), 7.68 (d, *J* = 8.3 Hz, 1H), 7.56 (dd, *J* = 8.4, 1.5 Hz, 1H), 7.24 (dd, *J* = 5.0, 3.8 Hz, 1H); ^{13}C-NMR (100 MHz, DMSO-d_6, at 90 ℃) δ 150.2, 141.9, 139.6, 132.7, 129.9, 128.4, 128.2, 125.7, 120.1, 119.8, 115.6, 104.3; ESI-HRMS: *m/z* calcd for $C_{12}H_7N_3S$ + H: 226.0433, found 226.0434.

*6-Methoxy-2-(thiophen-2-yl)-1H-benzo[d]imidazole (**1c**)* (1.15 g, 50%) pale yellow solid. mp 70-73 ℃ (decomposed); ^{1}H-NMR (400 MHz, DMSO-d_6) δ 12.80 (s, 1H), 7.78 (d, *J* = 3.8 Hz, 1H), 7.68 (d, *J* = 5.3 Hz, 1H), 7.45 (d, *J* = 5.3 Hz, 1H), 7.21 (q, *J* = 2.8 Hz, 1H), 7.05 (s, 1H), 6.83 (dd, *J* = 9.2, 2.3 Hz, 1H), 3.80 (s, 3H); ^{13}C-NMR (100 MHz, DMSO-d_6) δ 156.4, 134.5, 128.7, 126.6, 112.0, 56.0; ESI-HRMS: *m/z* calcd for $C_{12}H_{10}N_2OS$ + H: 231.0587, found 231.0593.

*2-(Furan-2-yl)-1H-benzo[d]imidazole (**2a**, **FBI**)* [47,48] (1.8236 g, 99%) brown solid. mp 271-273 ℃; ^{1}H-NMR (400 MHz, DMSO-d_6) δ 12.99 (s, 1H), 7.96 (q, *J* = 0.8 Hz, 1H), 7.56 (q, *J* = 3.1 Hz, 2H), 7.23-7.19 (m, 3H), 6.74-6.72 (m, 1H); ^{13}C-NMR (100 MHz, DMSO-d_6) δ 145.8, 145.3, 144.0, 139.2, 122.9, 115.5, 112.9, 111.3.

*2-(Furan-2-yl)-1H-benzo[d]imidazole-6-carbonitrile (**2b**)* (1.67 g, 80%) pale brown solid. mp 226-229 ℃; ^{1}H-NMR (400 MHz, DMSO-d_6) δ 13.46 (s, 1H), 8.07 (s, 1H), 7.99 (q, *J* = 0.8 Hz, 1H), 7.68 (d, *J* = 8.2 Hz, 1H), 7.56 (dd, *J* = 8.5, 1.5 Hz, 1H), 7.31 (dd, *J* = 3.4, 0.6 Hz, 1H), 6.74 (q, *J* = 1.7 Hz, 1H); ^{13}C-NMR (100 MHz, DMSO-d_6, at 90 ℃) δ 146.6, 145.4, 144.9, 141.6, 139.5, 125.7, 120.3, 119.8, 115.8, 112.5, 112.2, 104.4; ESI-

HRMS: *m/z* calcd for $C_{12}H_7N_3O$ + H: 210.0662, found 210.0664.

*2-(Furan-2-yl)-6-methoxy-1H-benzo[d]imidazole (**2c**)* (0.62 g, 29%) pale brown solid. mp 142-145 □ (decomposed); ^{1}H-NMR (400 MHz, DMSO-d_6) δ 12.78 (s, 1H), 7.91 (q, *J* = 0.8 Hz, 1H), 7.45 (d, *J* = 7.9 Hz, 1H), 7.13 (d, *J* = 4.0 Hz, 1H), 6.98 (s, 1H), 6.83 (dd, *J* = 8.9, 2.4 Hz, 1H), 6.70 (q, *J* = 1.7 Hz, 1H), 3.79 (s, 3H); ^{13}C-NMR (100 MHz, DMSO-d_6) δ 170.9, 156.5, 146.2, 144.8, 112.8, 112.3, 110.3, 55.9; ESI-HRMS: *m/z* calcd for $C_{12}H_{10}N_2O_2$ + H: 215.0815, found 215.0819.

2.3. Fluorescence-based screening of Ag^+-benzimidazole complexes

2.3.*1. Identification of excitation and emission wavelengths (λ_{ex}, λ_{em}) of candidate fluorophores*

Solutions of **1a-1c** and **2a-2c** in DMSO (25 μM, 10% DMSO) were added to pH 8.0 HEPES buffer (20 mM). Excitation and emission spectra of all candidates were recorded using a microplate reader.

2.3.2. Fluorescence-based screening of benzimidazole derivatives as ligands for silver ions

Solutions of benzimidazole derivatives **1a-1c** and **2a-2c** in DMSO (25 μM, 10% DMSO) were added to pH 8.0 HEPES buffer (20 mM). Ag^+ solutions (0-2.5 mM) in deionized distilled water were then added to give a final sample volume of 200 μL and 10% DMSO. The samples were mixed, incubated for 30 min at room temperature, and used for fluorescence intensity measurements. Fluorescence spectra were obtained using the λ_{ex} measured in section 2.3.1. (**1a**: λ_{ex} = 315 nm, **1b**: λ_{ex} = 323 nm, **1c**: λ_{ex} = 316 nm, **2a**: λ_{ex} = 307 nm, **2b**: λ_{ex} = 315 nm, **2c**: λ_{ex} = 323 nm).

2.3.3. Fluorescence-based screening of Ag^+-dye complexes as Cl^- probes

Solutions of benzimidazole derivatives **1a-1c** and **2a-2c** in DMSO (25 μM, 10% DMSO) were added to pH 8.0 HEPES buffer (20 mM). Ag^+ (125 μM) in deionized distilled water was added to the samples to give a final volume of 200 μL and 10% DMSO. The samples were then mixed and incubated for 30 min at room temperature. Solutions of Cl^- (0-1 mM) in deionized distilled water were added to the samples, which were then mixed, incubated for 10 min at room temperature, and used for fluorescence intensity measurements. Fluorescence spectra were obtained using the λ_{ex} measured in section 2.3.1. (**1a**: λ_{ex} = 315 nm, **1b**: λ_{ex} = 323 nm, **1c**: λ_{ex} = 316 nm, **2a**: λ_{ex} = 307 nm, **2b**: λ_{ex} = 315 nm, **2c**: λ_{ex} = 323 nm).

2.4. Optimization of conditions for preparing the Ag^+-FBI complex

*2.4.1. Preparation of Ag^+-**FBI** complexes and fluorescence analysis*

A solution of **FBI** in DMSO (25 μM) was adjusted to a pH of 7.4 using HEPES buffer (pH 7.4, 20 mM). Individual samples of the Ag^+-**FBI** complexes were prepared by adding $AgNO_3$ solutions (0-1 mM) in deionized distilled water to give a final sample volume of 1 mL and 10% DMSO. The Ag^+-**FBI** complexes were then incubated for 30 min at room temperature. These conditions were employed for the preparation of the Ag^+-**FBI** complex across all the experiments with only the concentration of the $AgNO_3$ solution being varied.

Fluorescence spectra (λ_{ex} = 307 nm) were recorded in triplicate, normalized, and the average value and error were calculated. This procedure was used for the remainder of the experiments unless otherwise stated.

2.4.2. Job's method (Job plot) [49,50]

To determine the binding stoichiometry, the binding mode of the Ag^+-**FBI** complex was investigated using the method of continuous variation (Job's method). The Job plot was obtained by plotting the difference in the fluorescence intensity at 344 nm (ΔF.I. = (F_0 – F) × [**FBI**]) against the mole fraction of the probe [Ag^+]/([**FBI**] + [Ag^+]). The resulting curve was fitted with non-linear curve parameters using OriginPro 2018b software.

2.4.3. Structural determination of the Ag^+-FBI complex using FT-IR and NMR studies

For FT-IR analysis, Ag^+-**FBI** complex samples were prepared as previously described using different equivalents of $AgNO_3$ (0, 0.5, 1, 3) and then lyophilized. FT-IR spectra were obtained using KBr pellets.

For NMR analysis, Ag^+-**FBI** complex samples were prepared by mixing **FBI** (100 mM) in DMSO-d_6 with different equivalents of $AgNO_3$ (0, 0.5, 1, 2, 3, 4, 5) in DMSO-d_6 and incubating for 30 min at room temperature.

2.5. Study of Ag^+-FBI complex as a fluorescent chemosensor of Cl^- ions

2.5.1. Effect of Cl^- ions on fluorescence

The Ag^+-**FBI** complex was prepared as described in section 2.4.1. using a 125 μM $AgNO_3$ solution. The mixture was stirred, incubated for 30 min at room temperature, and Cl^- solutions (0-10 mM) in deionized distilled water were added. The chloride ion-containing solutions were mixed and incubated for an additional 10 min at room temperature. The final sample preparation, spectral measurements, and data work-up were

performed as previously described.

2.5.2. Fluorescence response of chloride ion-ligand exchanged solutions at various pH

Ag^+-**FBI** samples were prepared as described in section 2.4.1. After adjusting the pH (pH range of 4.0–9.0), fluorescence spectra (λ_{ex} = 307 nm) were recorded.

Samples were prepared as described in section 2.5.1. using a 1 mM Cl^- solution. Measurements and data analysis were performed as previously described. The pH of the final samples was adjusted to between 4.0 and 9.0. Fluorescence spectra were used to examine the effect of ligand exchange on the fluorescence of the Ag^+-**FBI** complex.

2.5.3. Ionic constituent selectivity tests

Sample preparation, measurements, and data analysis were performed as described in section 2.5.1. with the following changes:

(a) Instead of a 1 mM Cl^- solution, samples were prepared using 100 µL of 1 mM solutions containing the following ionic constituents: Cl^- , I^- , Br^- , F^- , PO_4^{3-} , HCO_3^- , CH_3COO^- , SO_4^{2-} , NO_2^- , NO_3^- , ClO_4^- , Ca^{2+}, K^+, Mg^{2+}, Cd^{2+}, Cu^{2+}, Fe^{2+}, and Ni^{2+}.

(b) Samples were prepared using 100 µL of the following ionic constituents: [I^-] = 1 µM, [Br^-] = 1 µM, [F^-] = 1 µM, [PO_4^{3-}] = 20 µM, [HCO_3^-] = 200 µM, [CH_3COO^-] = 20 µM, [SO_4^{2-}] = 20 µM, [NO_2^-] = 1 mM, [NO_3^-] = 1 mM, [ClO_4^-] = 1 mM, [Ca^{2+}] = 250 µM, [K^+] = 500 µM, [Mg^{2+}] = 20 µM, [Cd^{2+}] = 1 µM, [Cu^{2+}] = 1 µM, [Fe^{2+}] = 1 µM, and [Ni^{2+}] = 1 µM.

2.5.4. Competing effect of ionic constituents

To determine the competing effects of other ions on chloride ion binding, the experiments described in sections 2.5.3. (a) and (b) were repeated with 1 mM Cl^- ion solution added to the samples.

2.5.5. Quantitative determination of chloride ions in artificial sweat

Sample preparation, measurements, and data analysis were performed as described in section 2.5.1. using 10 µL artificial sweat solution containing different chloride ion concentrations (20 mM, 50 mM, 100 mM). Artificial sweat solutions were prepared as previously described [51-53]. Quantitation was performed by comparing the fluorescence recovery of the artificial sweat treated samples with the results obtained from the

experiments in section 2.5.1. Chloride ion recovery was calculated by comparing the results with the estimated concentrations obtained from the experiments in section 2.5.1.

3. Results and discussion

3.1. Selection of optimal fluorescent chemosensor for chloride ions

To identify the optimal Cl^- ion fluorescent chemosensor, six different benzimidazole derivatives (**1a-c**, **2a-c**) with varying substituents at the C2 and C6 positions were synthesized and used as fluorescent ligands to prepare Ag^+ complexes. The fluorogenic response of the benzimidazole derivatives to Ag^+ ions and the Ag^+-benzimidazole complexes to chloride ions was then investigated (Figure 1). We first examined the change in fluorescence intensity of the six benzimidazole derivatives upon the addition of Ag^+. In the absence of Ag^+, all benzimidazole derivatives showed strong fluorescence peaks around 350 nm to 400 nm (Figure 1, Dye alone). Following the addition of Ag^+, fluorescence intensity decreased, with saturation occurring for 2-5 equivalents of Ag^+ within 30 minutes (Figure 1, Ag^+-Dye w/o Cl^- and Supporting Information). The quantum yields (Φ) of the benzimidazole derivatives and the Ag^+-benzimidazole complexes were also determined (Table S1). To investigate the recovery of fluorescence intensity of Ag^+-benzimidazole complexes in the presence of Cl^- ions, Cl^- ions were added to solutions of the complexes, resulting in a notable increase in the fluorescence of Ag^+-**1a** (~ 8 fold), Ag^+-**2a** (~ 11 fold), and Ag^+-**2c** (~ 7 fold) (Figure 1, Ag^+-Dye w/ Cl^-). This indicated that the fluorescence of the benzimidazole derivatives, which had been quenched upon complexation with Ag^+, was recovered through ligand exchange between the Ag^+-dye complex and the chloride ions. This exchange can be attributed to the strong affinity of Ag^+ for Cl^- ions forming AgCl. Based on these results, the Ag^+-**2a** complex (Ag^+-**FBI** complex) was chosen as the optimal probe for the detection of Cl^- ions.

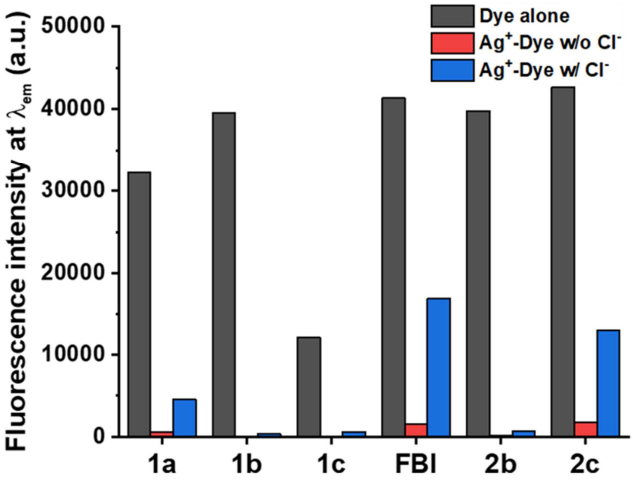

Figure 1. Fluorescence intensity of benzimidazole derivatives (**1a**-**1c**, **2a**-**2c**) complexed with Ag^+ and in the absence/presence of Cl^- ions. Ag^+-Dye complex: red bar, [Dye]:[Ag^+] = 25 μM:125 μM, 20 mM pH 8 HEPES, 10% DMSO. Ag^+-Dye complex with Cl^- : blue bar, [Dye]:[Ag^+]:[Cl^-] = 25 μM:125 μM:1 mM, 20 mM pH 8 HEPES, 10% DMSO. Measurements taken at the specific λ_{em} of each benzimidazole derivative.

3.2. Ag^+-FBI complex as fluorescent probe for chloride ions

The chemical structure of the Ag^+-**FBI** complex was determined by FT-IR and ^{1}H-NMR spectroscopy. The FT-IR spectra of free and complexed **FBI** showed a shift of the ν(C=N, benzimidazole) from 1420 cm^{-1} to 1385 cm^{-1} in the presence of Ag^+, indicating the involvement of the benzimidazole ring tertiary nitrogen in coordination (Figure S23) [54,55]. A comparison between the ^{1}H-NMR spectra of the free and complexed **FBI** showed a downfield shift for the benzimidazole –NH from 12.95 ppm in the presence of Ag^+ (Figure S24). In addition, the aryl and furanyl moieties signal at 7.6-7.0 ppm also shifted and displayed a distinct splitting pattern (Figure S24). These results suggest that the benzimidazole –NH remains intact during Ag^+ complexation and indicate that the furanyl ring is involved in the formation of the complex (Scheme 1, Fluorescence OFF structure) [56,57]. This was further confirmed by a Job plot, which revealed a 1:1 binding stoichiometry between Ag^+ and **FBI** (Figure S25).

To determine the Cl^- -sensing capacity of the Ag^+-**FBI** complex, the change in the fluorescence intensity of the complex was measured in the presence of various chloride ion concentrations (Figure 2). Since the decrease in the fluorescence intensity of **FBI** by Ag^+ was saturated with 5 equivalents of Ag^+, 25 μM **FBI** and 125 μM Ag^+ were used to prepare the Ag^+-**FBI** complex in a pH 7.4 HEPES buffer solution containing 10% DMSO (Figure S26). The fluorescence intensity of the Ag^+-**FBI** complex increased linearly with increasing

chloride ion concentration up to 1.5 mM (Figure 2b). The limit of detection (LOD) for chloride ions was determined to be 19 μM based on the 3σ/slope (Figure 2b; σ 3.441), which is lower than for the majority of previously reported Cl^- probes. Most importantly, this detection limit is below the maximum concentration of chloride ions in sweat, indicating that our Ag^+-**FBI** complex could be used for quantifying chloride ions in sweat without interference from the biological matrix.

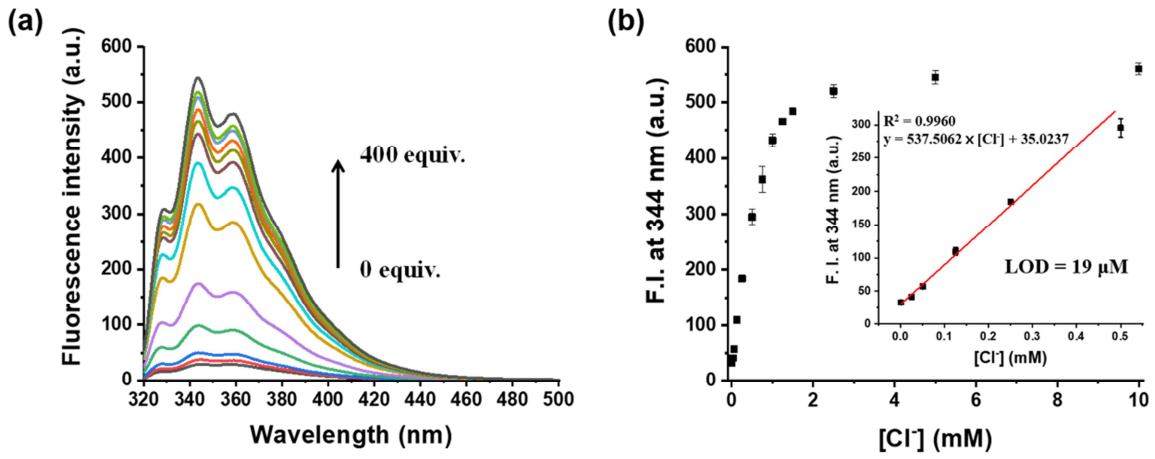

Figure 2. (a) Fluorescence spectra for incremental increases in chloride ion concentration ([**FBI**]:[Ag^+] = 25 μM:125 μM). **(b)** Plot of the fluorescence intensity at 344 nm of Ag^+-**FBI** ([**FBI**]:[Ag^+] = 25 μM:125 μM) versus the concentration of Cl^- (20 mM pH 7.4 HEPES, 10% DMSO, λ_{ex} = 307 nm). F.I.: Fluorescence intensity. LOD: Limit of detection.

Since sweat is composed of various ionic constituents, it is essential that the Ag^+-**FBI** complex displays a high selectivity for chloride ions to be applicable for sweat-related applications. Both anions and metal cations are constituents of sweat, and the effect of these ions on the detection of Cl^- was examined. It should be noted that, in physiological conditions, the concentrations of these other ions in sweat are much lower than the level of chloride ion [15,51]. Though some of ion species at high concentrations were found to interfere with the response of the Ag^+-**FBI** complex (Figure S27), in physiological conditions, other ions except for Cl^- induced negligible change in fluorescence intensity of Ag^+-**FBI** complex. These results demonstrated that Ag^+-**FBI** complex exhibits high selectivity toward Cl^- , suggesting that Ag^+-**FBI** should be applicable for detecting chloride ions in sweat, despite its contamination with other biological constituents.

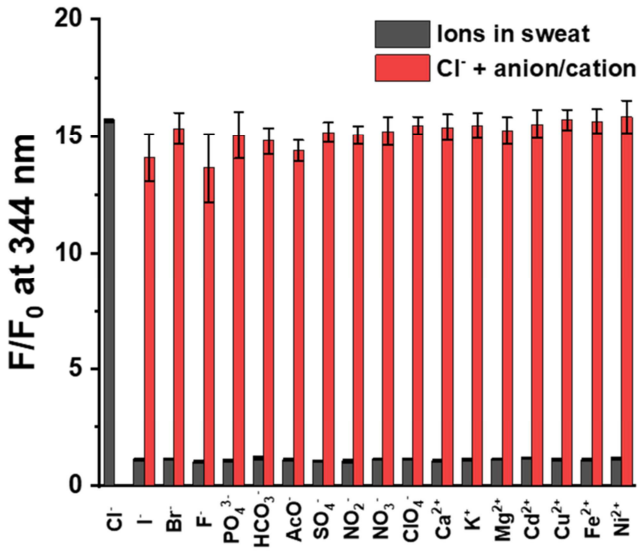

238

239 **Figure 3.** Change in fluorescence intensity of Ag^+-**FBI** ([**FBI**]:[Ag^+] = 25 μM:125 μM) in the presence of
240 biologically relevant ions, [Cl^-] = 1 mM, [I^-] = 1 μM, [Br^-] = 1 μM, [F^-] = 1 μM, [PO_4^{3-}] = 20 μM,
241 [HCO_3^-] = 200 μM, [CH_3COO^-] = 1 mM, [SO_4^{2-}] = 1 mM, [NO_2^-] = 1 mM, [NO_3^-] = 1 mM, [ClO_4^-] = 1
242 mM, [Ca^{2+}] = 250 μM, [K^+] = 500 μM, [Mg^{2+}] = 20 μM, [Cd^{2+}] = 1 μM, [Cu^{2+}] = 1 μM, [Fe^{2+}] = 1 μM, [Ni^{2+}] =
243 1 μM, (20 mM pH 7.4 HEPES, 10% DMSO, λ_{ex} = 307 nm). F: fluorescence intensity. F_0: fluorescence intensity
244 of Ag^+-**FBI** in the absence of ions.

245 The effect of pH on chloride ion detection was investigated in the pH range of 4.0-9.0 (Figure 4). It is
246 worth noting that while the Ag^+-**FBI** complex functioned well across a pH range of 6.0-8.0, the strongest
247 response to chloride ions was observed at the biologically relevant pH of 7.4. This finding suggests that the Ag^+-
248 **FBI** complex is applicable to chloride ion detection in physiological conditions.

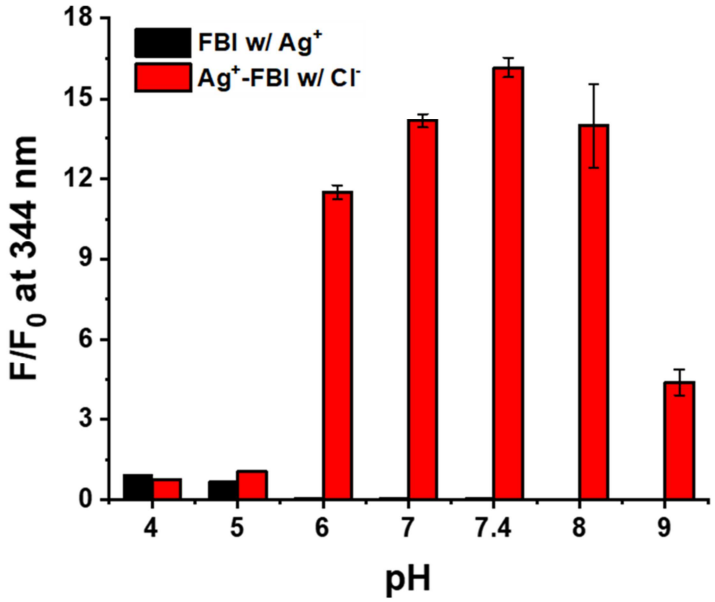

Figure 4. Change of fluorescence intensity of **FBI** with silver ions (black bar; [**FBI**]:[Ag^+] = 25 μM:125 μM). Change of fluorescence intensity of Ag^+-**FBI** complex in the presence of chloride ions (red bar; [**FBI**]:[Ag^+]:[Cl^-] = 25 μM:125 μM:1 mM). Conditions: 20 mM pH buffer, 10% DMSO, λ_{ex} = 307 nm. F: fluorescence intensity. F_0: fluorescence intensity of control.

3.3. Quantitative determination of chloride ions in artificial sweat

To evaluate the suitability of the Ag^+-**FBI** complex to detect chloride ions in sweat samples for the diagnosis of CF, the chloride ion level of artificial sweat samples was determined (Table 1). Three artificial sweat samples with different chloride ion concentrations were prepared following the British Standard (BS EN1811-1999). Chloride ion concentrations were selected with respect to the diagnostic reference level for cystic fibrosis in adults: < 40 mM (negative), 40–59 mM (possible), and > 60 mM (positive), with slightly lower values for infants. Chloride ion recoveries ranged from 98 to 114%, with the relative standard deviation (RSD) ranging between 4.55 to 7.22% (Table 1). These results indicate that the Ag^+-**FBI** complex accurately detects chloride ions in complex artificial sweat samples, suggesting that this probe has great potential for use in the sweat test diagnosis of cystic fibrosis.

Table 1. Detection and quantitation of Cl^- in artificial sweat samples.

[Cl^-]	Recovery (%)	RSD[a] (%) (n=3)	Relative error (%)
20 mM	109 ± 3	4.55	2.63

50 mM	114 ± 5	6.97	4.02
100 mM	98 ± 4	7.22	4.17

[a] Relative standard deviation.

4. Conclusions

We developed an Ag^+-benzimidazole complex-based chloride ion chemosensor, Ag^+-**FBI**, by exploiting the strong interaction between Ag^+ and Cl^- ions. The fluorescence intensity of the Ag^+-**FBI** complex increased in the presence of Cl^- ions and allowed for the sensitive (LOD = 19 μM) and rapid (response time < 3 min) detection of Cl^- ions. In addition, the Ag^+-**FBI** complex showed high selectivity toward Cl^- ions and was unaffected by other common ionic constituents in sweat. Notably, the chemosensor worked effectively in the pH range of 6.0-8.0 with peak performance at the biologically relevant pH of 7.4 and chloride ions in complex artificial sweat samples were quantitatively measured. The Ag^+-**FBI** complex is a simple and effective chloride ion chemosensor and is expected to have clinical applications for quantifying chloride ions in diagnostic sweat tests.

Acknowledgements

This work was supported by GIST Research Institute(GRI) grant funded by the GIST in 2019 and the National Research Foundation of Korea (NRF) grant funded by the Korea government(MSIT) (NRF-2018R1A4A1024963).

Appendix A. Supplementary data

Supplementary data related to this article can be found at doi ****

References

[1] Jentsch TJ, Stein V, Weinreich F, Zdebik AA. Molecular Structure and Physiological Function of Chloride Channels. Physiol Rev 2002;82:503–68. https://doi.org/10.1152/physrev.00029.2001

[2] Sweeney DW, Granade GV, Eversmeyer MG, Whitney DA. Phosphorous, Potassium, Chloride, and Fungicide Effects on Wheat Yield and Leaf Rust Severity. J Plant Nutr 2000;23:1267–81. https://doi.org/10.1080/01904160009382099.

[3] Iniesta J, González-García J, Expósito E, Montiel V, Aldaz A. Influence of chloride ion on electrochemical

289 degradation of phenol in alkaline medium using bismuth doped and pure PbO_2 anodes. Wat Res 2001;35:3291–
290 300. https://doi.org/10.1016/S0043-1354(01)00043-4.

291 [4] Steffensen I-L, Frolich W, Dahl KH, Iversen PO, Lyche JL, Lillegaard ITL, Alexander J. Benefic and risk
292 assessment of increasing potassium intake by replacement of sodium chloride with potassium chloride in
293 industrial food products in Norway. Food Chem Toxicol 2018;111:329–40.
294 https://doi.org/10.1016/j.fct.2017.11.044.

295 [5] LeGrys VA. Sweat testing for the diagnosis of cystic fibrosis: Practical considerations. J Pediatr
296 1996;129:892–7. https://doi.org/10.1016/s0022-3476(96)70034-3.

297 [6] LeGrys VA. Assessment of Sweat-Testing Practices for the Diagnosis of Cystic Fibrosis. Arch Pathol Lab
298 Med. 2001;125:1420–4. https://doi.org/10.1043/0003-9985(2001)125<1420:AOSTPF>2.0.CO;2.

299 [7] Puljak L, Kilic G. Emerging roles of chloride channels in human diseases. Biochim Biophys Acta-Mol Basis
300 Dis 2006;1762:404–13. https://doi.org/10.1016/j.bbadis.2005.12.008.

301 [8] LeGrys VA, Yankaskas JR, Quittell LM, Marshall BC, Mogayzel Jr PJ. Diagnostic Sweat Testing: The
302 Cystic Fibrosis Foundation Guidelines. J Pediatr 2007;151:85–9. https://doi.org/10.1016/j.jpeds.2007.03.002.

303 [9] Riordan JR, Rommens JM, Kerem B-S, Alon N, Rozmahel R, Grzelczak Z, Zielenski J, Lok S, Plavsic N,
304 Chou J-L, Drumm ML, Iannuzzi MC, Collins FS, Tsui L-C. Identification of the Cystic Fibrosis Gene: Cloning
305 and Characterization of Complementary DNA. Science 1989;245:1066–73.
306 https://doi.org/10.1126/science.2475911.

307 [10] Sheppard DN, Welsh MJ. Structure and Function of the CFTR Chloride Channel. Physiol Rev
308 1999;79:S23–45. https://doi.org/10.1152/physrev.1999.79.1.S23.

309 [11] López-Ruiz B. Advances in the determination of inorganic anions by ion chromatography. J Chromatogr A
310 2000;881:607–27. https://doi.org/10.1016/S0021-9673(00)00244-2.

311 [12] Shishkanova TV, Sýkora D, Sessler JL, Král V. Potentiometric response and mechanism of anionic
312 recognition of heterocalixarene-based ion selective electrodes. Anal Chim Acta 2007;587:247–53.
313 https://doi.org/10.1016/j.aca.2007.01.044.

314 [13] Kimmel DW, LeBlanc G, Meschievitz ME, Cliffel DE. Electrochemical Sensors and Biosensors. Anal

315 Chem 2012;84:685–707. https://doi.org/10.1021/ac202878q.

316 [14] Toh HS, Batchelor-McAuley C, Tschulik K, Compton RG. Electrochemical detection of chloride levels in
317 sweat using silver nanoparticles: a basis for the preliminary screening for cystic fibrosis. Analyst
318 2013;138:4292–7. https://doi.org/10.1039/c3an00843f.

319 [15] Lopez-Moreno C, Perez IV, Urbano AM. Development and validation of an ionic chromatography method
320 for the determination of nitrate, nitrite and chloride in meat. Food Chem 2016;194:687–94.
321 https://doi.org/10.1016/j.foodchem.2015.08.017.

322 [16] Cunha-Silva H, Acros-Martinez J. Development of a selective chloride sensing platform using a screen-
323 printed platinum electrode. Talanta 2019;195:771–7. https://doi.org/10.1016/j.talanta.2018.12.008.

324 [17] Bai Y, Zhang B-G, Xu J, Duan C-Y, Dang D-B, Liu D-J, Meng Q-J. Conformational switching fluorescent
325 chemosensor for chloride anion. New J Chem 2005;29:777–9. https://doi.org/10.1039/B500252D.

326 [18] Schazmann B, Alhashimy N, Diamond D. Chloride Selective Calix[4]arene Optical Sensor Combining
327 Urea Functionality with Pyrene Excimer Transduction. J Am Chem Soc 2006;128:8607–14.
328 https://doi.org/10.1021/ja061917m.

329 [19] Wu J-S, Wang P-F, Zhang X-H, Wu S-K. An efficient chloride-selective fluorescent chemosensor based on
330 2,9-bis(4'-hydroxyphenyl)phenanthroline Cu(II) complex. Spectroc Acta Pt A 2007;67:281–6.
331 https://doi.org/10.1016/j.saa.2006.07.021.

332 [20] Tavallali H, Rad GD, Parhami A, Abbasiyan E. Colorimetric detection of copper and chloride in
333 DMSO/H_2O media using bromopyrogallol red as a chemosensor with analytical applications. Spectroc Acta Pt
334 A-Molec Biomolec Spectr 2012;97:60–5. https://doi.org/10.1016/j.saa.2012.05.071.

335 [21] Kaur A, Sharma H, Kaur S, Singh N, Kaur N. A counterion displacement assay with a Biginelli product: a
336 ratiometric sensor for Hg^{2+} and the resultant complex as a sensor for Cl^-. RSC Advances 2013;3:6160–6.
337 https://doi.org/10.1039/c3ra40236c.

338 [22] Dorazco-Gonzalez A. Chemosensing of Chloride Based on a Luminescent Platinum(II) NCN Pincer
339 Complex in Aqueous Media. Organometallics 2014;33:868–75. https://doi.org/10.1021/om4007054.

340 [23] Bazany-Rodríguez I, Martínez-Otero D, Barroso-Flores J, Yatsimirsky AK, Dorazco-González A. Sensitive

341 water-soluble fluorescent chemosensor for chloride based on a bisquinolinium pyridine-dicarboxamide
342 compound. Sens Actuator B-Chem 2015;221:1348–55. https://doi.org/10.1016/j.snb.2015.07.031.

343 [24] Chilbac AL, Roman G, Cojocaru C, Sacarescu G, Simionescu M, Sacarescu L. Pyrazoline based chloride
344 sensor for body fluids screening. J Mol Liq 2019;284:139–46. https://doi.org/10.1016/j.molliq.2019.04.007.

345 [25] Tong L, Sun S, Qiao M, Fan J, Ding L. Selective turn-on sensing of Cu^{2+} and Cl^- by a ferrocene-modified
346 pyrene derivative. J Photochem Photobiol A-Chem 2019;374:131-7.
347 https://doi.org/10.1016/j.jphotochem.2019.01.036.

348 [26] Li P, Xie T, Fan N, Li K, Tang B. Ratiometric fluorescence imaging for distinguishing chloride
349 concentration between normal and ischemic ventricular myocytes. Chem Commun 2012;48:2077–9.
350 https://doi.org/10.1039/C1CC15258K.

351 [27] Kim JP, Xie Z, Creer M, Liu Z, Yang J. Citrate-based fluorescent materials for low-cost chloride sensing in
352 the diagnosis of cystic fibrosis. Chem Sci 2017;8:550–8. https://doi.org/10.1039/c6sc02962k.

353 [28] Zhang F, Ma C, Wang Y, Liu W, Liu X, Zhang H. Fluorescent probes for chloride ions in biological samples.
354 Spectroc Acta Pt A-Molec Biomolec Spectr 2018;205:428–34. https://doi.org/10.1016/j.saa.2018.07.060.

355 [29] Vallejos S, Hernando E, Trigo M, Garcia FC, Garcia-Valverde M, Iturbe D, Cabero MJ, Quesada R, Garcia
356 JM. Polymeric chemosensor for the detection and quantification of chloride in human sweat. Application to the
357 diagnosis of cystic fibrosis. J Mater Chem B 2018;6:3735–41. https://doi.org/10.1039/c8tb00682b.

358 [30] Ma C, Zhang F, Wang Y, Zhu X, Liu X, Zhao C, Zhang H. Synthesis and application of ratio fluorescence
359 probe for chloride. Anal Bioanal Chem 2018;410:6507–16. https://doi.org/10.1007/s00216-018-1250-0.

360 [31] Jonte JH, Martin Jr DS. The Solubility of Silver Chloride and the Formation of Complexes in Chloride
361 Solution. J Am Chem Soc 1952;74:2052–4.

362 [32] Harris DC. Quantitative Chemical Analysis. 8th ed. W.H. Freeman Custom Publishing; 2010.

363 [33] Meija J. Mohr's method challenge. Anal Bioanal Chem 2016;408:1721–2. https://doi.org/10.1007/s00216-
364 015-9273-2.

365 [34] Dean KES, Klein G, Renaudet O, Reymond J-L. A Green Fluorescent Chemosensor for Amino Acids
366 Provides a Versatile High-Throughput Screening (HTS) Assay for Protease. Bioorg Med Chem Lett

2003;13:1653-6. https://doi.org/10.1016/S0960-894X(03)00280-4.

[35] Chen Y, Chen J, Ma K, Cao S, Chen X. Fluorimetric determination of phytic acid in urine based on replacement reaction. Anal Chim Acta 2007;605:185–91. https://doi.org/10.1016/j.aca.2007.10.041.

[36] Lou X, Zhang L, Qin J, Li Z. An alternative approach to develop a highly sensitive and selective chemosensor for the colorimetric sensing of cyanide in water. Chem Commun 2008;5848–50. https://doi.org/10.1039/B812746H.

[37] Choi MG, Cha S, Lee H, Jeon HL, Chang S-K. Sulfide-selective chemosignaling by a Cu^{2+} complex of dipicolylamine appended fluorescein. Chem Commun 2009;7390–2. https://doi.org/10.1039/B916476F.

[38] Jung HS, Han JH, Habata Y, Kang C, Kim JS. An iminocoumarin-Cu(II) ensemble-based chemodosimeter toward thiols. Chem Commun 2011;47:5142-4. https://doi.org/10.1039/c1cc10672d.

[39] Kittiloespaisan E, Takashima I, Kiatpathomchai W, Wongkongkatep J, Ojida A. Coordination ligand exchange of a xanthene probe-Ce(III) complex for selective fluorescence sensing of inorganic pyrophosphate. Chem Commun 2014;50:2126–8. https://doi.org/10.1039/c3cc48101h.

[40] Eom MS, Noh J, Kim H-S, Yoo S, Han MS, Lee S. High-Throughput Screening Protocol for the Coupling Reactions of Aryl Halides Using a Colorimetric Chemosensor for Halide Ions. Org Lett 2016;18:1720-3. https://doi.org/10.1021/acs.orglett.6b00300.

[41] Lee S, Kang S, Eom MS, Han MS. Colorimetric assay for β-lactamase activity using cocktail of penicillin and 4-(2-pyridylazo)resorcinol (PAR)-$2Hg^{2+}$ complex. Dyes Pigment 2017;137:518-22. https://doi.org/10.1016/j.dyepig.2016.10.026.

[42] McCann M, Curran R, Ben-Shoshan M, McKee V, Devereux M, Kavanagh K, Kellett A. Synthesis, structure and biological activity of silver(I) complexes of substituted imidazoles. Polyhedron 2013;56:180–8. https://doi.org/10.1016/j.poly.2013.03.057.

[43] Wang XX, Liu YG, Hecke KV, Goltsev A, Cui GH. Three Silver(I) Coordinatino Polymers Constructed from Flexible Bis(benzimidazole) and Carboxylates Ligands. Z Anorg Allg Chem 2015;641:903–10. https://doi.org/10.1002/zaac.201400597.

[44] Haque RA, Choo SY, Budagumpi S, Iqbal MA, Abdullah AA. Silver(I) complexes of mono- and bidentate

393 N-heterocyclic carbine ligands: Synthesis, crystal structures, and in vitro antibacterial and anticancer studies.
394 Eur J Med Chem 2015;90:82–92. https://doi.org/10.1016/j.ejmech.2014.11.005.

395 [45] Kalinowska-Lis U, Felczak A, Chęcińska L, Szabłowska-Gadomska I, Patyna E, Małecki M, Lisowska K,
396 Ochocki J. Antibacterial Activity and Cytotoxicity of Silver(I) Complexes of Pyridine and (Benz)Imidazole
397 Derivatives. X-ray Crystal Structure of $[Ag(2,6\text{-di}(CH_2OH)py)_2]NO_3$. Molecules 2016;21:87–100.
398 https://doi.org/10.3390/molecules21020087.

399 [46] Liang X, Luan S, Yin Z, He M, He C, Yin L, Zou Y, Yuan Z, Lixia Y, Song X, Lv C, Zhang W. Recent
400 advances in the medical use of silver complex. Eur J Med Chem 2018;157:62–80.
401 https://doi.org/10.1016/j.ejmech.2018.07.057.

402 [47] Jiang Y-Q, Jia S-H, Sun Y-M, Li Wei, Zhang W-W, Xu G-Q. An efficient $NaHSO_3$-promoted protocol for
403 chemoselective synthesis of 2-substituted benzimidazoles in water. Chem Pep 2018;72:1265–76.
404 https://doi.org/10.1007/s11696-017-0367-5.

405 [48] Xiang S-K, Tan W, Zhang D-X, Tian X-L, Feng C, Wang B-Q, Zhao K-Q, Hu P, Yang H. Synthesis of
406 benzimidazoles by potassium *tert*-butoxide-promoted intermolecular cyclization reaction of 2-iodoanilines with
407 nitriles. Org Biomol Chem 2013;11:7271–5. https://doi.org/10.1039/c3ob41479e.

408 [49] Valeur B. Molecular Fluorescence: Principles and Applications. Wiley-VCH Verlag GmbH; 2001.

409 [50] Huang S, He S, Lu Y, Wei F, Zeng X, Zhao L. Highly sensitive and selective fluorescent chemosensor for
410 Ag^+ based on a coumarin-Se_2N chelating conjugate. Chem Commun 2011;47:2408–10.
411 https://doi.org/10.1039/C0CC04589F.

412 [51] Stefaniak AB, Harvey CJ. Dissolution of materials in artificial skin surface film liquids. Toxicol Vitro
413 2006;20:1265–83. https://doi.org/10.1016/j.tiv.2006.05.011.

414 [52] Kulthong K, Srisung S, Boonpavanitchakul K, Kangwansupamonkon W, Maniratanachote R.
415 Determination of silver nanoparticle release from antibacterial fabrics into artificial sweat. Part Fibre Toxicol
416 2010;7:8–16. https://doi.org/10.1186/1743-8977-7-8.

417 [53] Callewaert C, Buysschaert B, Vossen E, Fievez V, Van de Wiele T, Boon N. Artificial sweat composition to
418 grow and sustain a mixed human axillary microbiome. J Microbiol Methods 2014;103:6–8.

https://doi.org/10.1016/j.mimet.2014.05.005.

[54] Galal SA, Hegab KH, Hashem AM, Youssef NS. Synthesis and antitumor activity of novel benzimidazole-5-carboxylic acid derivatives and their transition metal complexes as topoisomerase II inhibitors. Eur J Med Chem 2010;45:5685-91. https://doi.org/10.1016/j.ejmech.2010.09.023.

[55] Haque RA, Iqbal MA, Khadeer Ahamed MB, Majid AA, Hameed ZAA. Design, synthesis and structural studies of *meta*-xylyl linked *bis*-benzimidazolium salts: potential anticancer agents against 'human colon cancer'. Chem Cent J 2012;6:68-81. https://doi.org/10.1186/1752-153X-6-68.

[56] Fisher CM, Fuller E, Burke BP, Mogilireddy V, Pope SJA, Sparke AE, Déchamps-Olivier I, Cadiou C, Chuburu F, Faulkner S, Archibald SJ. A benzimidazole functionalized DO3A chelator showing pH switchable coordination modes with lanthanide ions. Dalton Trans 2014;43:9567–78. https://doi.org/10.1039/c4dt00519h.

[57] Majumdar A, Mondal S, Daniliuc CG, Sahu D, Ganguly B, Ghosh S, Ghosh U, Ghosh K. α-Amino Acid Derived Benzimidazole-Linked Rhodamines: A Case of Substitution Effect at the Amino Acid Site toward Spiro Ring Opening for Selective Sensing of Al^{3+} Ions. Inorg Chem 2017;56:8889−99. https://doi.org/10.1021/acs.inorgchem.7b00835.

Highlights

- Ag^{+}–benzimidazole (**FBI**) complex was developed as fluorescent chemosensor for Cl^{-} .
- The probe exhibited high selectivity and sensitivity toward Cl^{-} (detection limit 19 μM).
- The probe was successfully applied to the detection of Cl^{-} in artificial sweat.

Declaration of interests

☒ The authors declare that they have no known competing financial interests or personal relationships that could have appeared to influence the work reported in this paper.

☐ The authors declare the following financial interests/personal relationships which may be considered as potential competing interests: